Thin Solid Films 693 (2020) 137677

Contents lists available at ScienceDirect

Thin Solid Films

journal homepage: www.elsevier.com/locate/tsf

A facile strategy for the preparation of hybrid copper nanowire-TiO_2 film

Liangjing Shi, Ranran Wang, Yangqiao Liu, Jing Sun*

State Key Laboratory of High Performance Ceramics and Superfine Microstructure, Shanghai Institute of Ceramics, Chinese Academy of Sciences, 585 Heshuo Road, Shanghai 201899, China

ARTICLE INFO

Keywords:
Carrier density
Copper nanowires
Stability
Thin films
Titanium dioxide

ABSTRACT

In this study, hybrid copper nanowire-TiO_2 film was prepared through a simple hydrogen treatment. In the hydrogenation process, oxygen vacancies and surface hydroxyl groups were formed on TiO_2 at the temperature of 400°C due to the facilitation of copper nanowires. Mott-Schottky measurements revealed that the carrier density of hybrid film was enhanced by 25.3 times compared to no hydrogenation film. In addition, stability test of the hybrid films shows that TiO_2 layer can also protect the underlying copper nanowires from oxidation. This kind of copper nanowire-TiO_2 film with improved carrier density might be used as electrodes of solar cells or materials for photo catalysis.

1. Introduction

Titanium dioxide (TiO_2) is one of the most important semiconductors due to its excellent physicochemical properties as well as its nontoxicity, low cost and environmental friendliness [1]. In 1972, Fujishima groups found a useful method of water photolysis by using TiO_2 and Pt [2]. Since then, more and more research have been reported about the development of TiO_2 materials, which led to many promising applications in areas ranging from solar cells, photochromic and electrochromic devices to photocatalytic devices [3–7]. However, large band gap energy of TiO_2 (3.2 eV) limits its utilization of sunlight, and only about 5% solar energy can be captured by TiO_2. Moreover, the intrinsic conductivity of TiO_2 is about 10^{-10} S/cm, which cannot realize the efficient separation and transportation of photo-generated charge carriers [8,9]. Therefore, it is important to fundamentally improve the morphology and electronic structure of TiO_2 for effective separation and transportation of photo-generated electron and hole. Oxygen deficiency, on the surface of the molecular structure of TiO_2, is one of the important active centers. An enormous number of investigations have been attempted to enhance the photo electrochemical performance of TiO_2 by adjusting the oxygen deficiency, which result in the fabrication of nonstoichiometric TiO_2. Diebold [10] revealed that oxygen vacancy, which generated after hydrogenating TiO_2 under high temperature and low pressure for a long time, could act as a special intermediate absorption band. Chen et al. [11] reported that the color of TiO_2 would change from white to black by long time hydrogen treatment, and this transformation not only enhanced the visible light absorption range, but also improved the photo-catalytic effect. This black TiO_2 has attracted numerous attentions [11–14]. Huang et al. [15] revealed that aluminum (Al) could help to obtain the oxygen-deficient TiO_{2-x} powders with improved wide-spectrum light absorption and photo electrochemical performance in hydrogen environment with pressure as low as 0.5 Pa. However, the reported methods for synthesizing nonstoichiometric TiO_2 all require harsh conditions such as high temperature (>500 °C), time consuming on fabrication (from several hours to a few days), and low pressure environment (<0.5 Pa). Therefore, it is of great significance to explore a simple and efficient procedure to synthesize nonstoichiometric TiO_2 with improved performance.

In this study, a facile method to fabricate TiO_2 thin film via the assistance of copper nanowires (Cu NWs) has been reported. Over the past decades, metal-assisted TiO_2 nano-materials have been widely studied to improve photo-electrochemical performance. Many kinds of metals, for example, Au, Ag, Pt, Cu, can promote photo-electrochemical activity of TiO_2 by the visible light-induced charge transfer from metals to TiO_2. Nano-scale metal nanowires have much higher chemical activity than that of metal particles. Copper is cheaper than aforementioned metals and Cu NWs exhibits great application potential in photo-electrochemical fields because of the favorable electronic transmission properties [16–18]. We demonstrated that Cu NWs can effectively promote the formation of oxygen vacancies and hydroxyl group on TiO_2 by H_2 treatment at atmospheric pressure, and the temperature was only 400 °C with short processing time (1 h). The obtained hybrid film exhibited greatly higher carrier density than that of pristine ones and upper-layer TiO_2 can also played an important role in protecting the underlying Cu NWs.

* Corresponding authors.
E-mail address: jingsun@mail.sic.ac.cn (J. Sun).

https://doi.org/10.1016/j.tsf.2019.137677
Received 5 December 2018; Received in revised form 22 October 2019; Accepted 28 October 2019
Available online 31 October 2019
0040-6090/

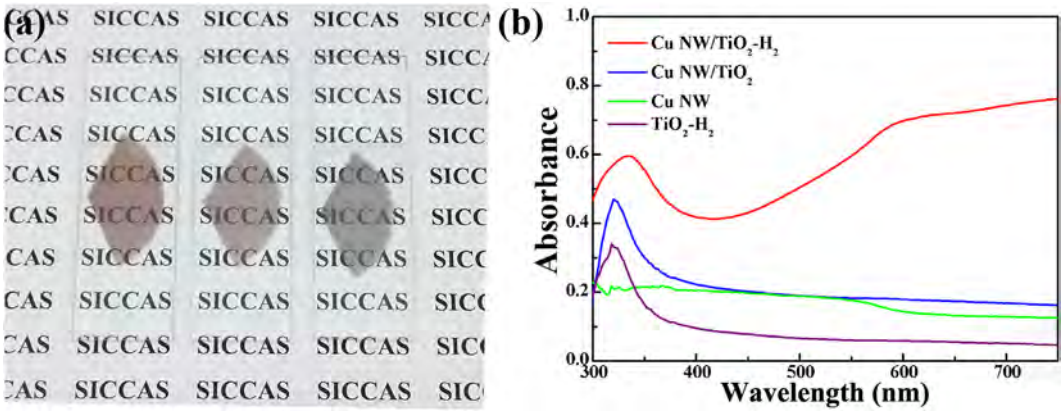

Fig. 1. (a) Digital photograph picture of pristine Cu NW film (left), Cu NW/TiO_2 film (middle) and black Cu NW/TiO_2−H_2 film (right). (b) UV–vis absorption spectra of the Cu NW/TiO_2−H_2, Cu NW/TiO_2, Cu NW and TiO_2−H_2.

2. Methods

2.1. TiO_2 precursor synthesis

TiO_2 precursor was prepared by a simple sol-gel method, as described previously [19]. 20 mL of absolute ethanol and 5 mL of titanium n-butoxide ($Ti(OBu)_4$) were mixed up to form solution A. Then the mixture solution B with 1.5 mL of deionized water, 10 mL of absolute ethanol and 1.5 mL of glacial acetic acid was dropwise added into solution A under continuous stirring. The obtained homogeneous white sol was magnetically stirred continuously for 12 h at room temperature.

2.2. Fabrication of cu NWs on substrates

Cu NWs were fabricated according to the procedure proposed by our group [20,21]. Hexadecylamine and Cetyltrimethyl Ammonium Bromide were firstly mixed at elevated temperature to form a liquid-crystalline medium. Upon addition of copper acetylacetonate, ultra-long nanowires with excellent dispersibility formed spontaneously with Pt as catalyst. The films were prepared by a vacuum filtration method. Typically, Cu NWs were dispersed in toluene by bath sonication for 1–2 min, and then filtered onto a nitrocellulose filter membrane. After filtration, the membranes were transferred onto a glass substrate, dried under vacuum at 80 °C for 2 h, and then dipped in acetone for 30 min to dissolve the filtration membrane. Cu NWs films formed on the substrate. Finally, the films were treated under hydrogen gas at 300 °C to remove the oxidized layers of copper and the residue organics from the surface.

2.3. Fabrication of black TiO_2films on cu NWs film

The TiO_2 sol was spin-coated onto the Cu NWs films mentioned before at the speed of 5000 rpm for 30 s to form uniform Cu NW/TiO_2 film. Then the film was annealed at 400 °C for 1 h under the protection of hydrogen gas (100 sccm). After cooling down naturally, the H_2 treated Cu NW/TiO_2 film (Cu NW/TiO_2-H_2) was obtained. For comparison, hydrogen treated TiO_2 film was also fabricated. The TiO_2 sol was spin-coated onto the glass or F-doped Tin Oxide substrate at the speed of 5000 rpm for 30 s to form the uniform TiO_2 film. Then the film was annealed at 400 °C for 1 h under the protection of hydrogen gas (100 sccm). After cooling down naturally, the H_2 treated TiO_2 film (TiO_2−H_2) was obtained.

2.4. Electrochemical performance characterization

Photo-electrochemical performance measurements were performed in a typical three-electrode system. The Cu NW/TiO_2−H_2 film and comparative films were fabricated on the F-doped Tin Oxide substrate as the photoanodes. The substrate edges were sealed with insulating epoxy resin. The working electrode area was in the range of 0.7–1.0 cm^2. 1 M NaOH aqueous solution (pH = 13.6) was used as an electrolyte for measurement. A solar simulator (AM 1.5, Newport) with an irradiation intensity of 100 mW/cm^2 was used as the illumination source. Linear sweeps were measured by a CHI 660D electrochemical station, with Ag/AgCl as reference and Pt wire as counter electrodes in a range of −1 V to 0.5 V, and the scan rate was 10 mV/s. The measurements were done with the front side illumination. Mott-Schottky plots were measured at a frequency of 5000 Hz by the same CHI 660D electrochemical station with a 0.1 M Na_2SO_4 aqueous solution.

2.5. Material characterization

Morphological observation was carried out on transmission electron microscope (TEM, JEM-2100F at 200 kV). Optical transmittances of the films were measured using Perkin Elmer Lambda 950 UV–vis spectrometer. XPS spectra were observed with a Thermo Scientific ESCALAB 250Xi X-ray Photoelectron Spectrometer to measure the atom species. Mono Al Kα(1486.6 eV) was used, and currently beam energy is 1 kV × 1μA with 1 × 1mm^2 spot size. Analysis of the binding energy is based on the result of references [22,23]. Deconvolution of XPS spectra were resolved by fitting each peak (peak type: s, Full Width at Half Maxima < 2.7 eV) with a constrained Guassian-Lorentzian function (L/G = 20%) after background subtraction (backgroud type: shirley). Raman measurements were carried out on a Raman microscope (Thermo Scientific Raman DXR) by using a 532 nm laser under ambient conditions, the laser spot size and power were ~0.7 μm and 8 mW, respectively.

3. Result and discussion

Fig. 1(a) illustrates the photograph of Cu NW/TiO_2−H_2 films, Cu NW/TiO_2 and pristine Cu NW films. The film color changed from grey red to black after hydrogen treatment. The dark color reveals that the visible light absorption of TiO_2 films changed because of hydrogen treatment. The absorbance spectra of pristine Cu NW with and without TiO_2 are similar, except the sharp peak at ~320 nm, which is attributed to the intrinsic band-gap absorption of TiO_2. From Fig. 1(b), the black Cu NW/TiO_2–H_2 films have an obvious photo absorption from UV light to visible light region, compared with Cu NW/TiO_2 and TiO_2−H_2 films. Therefore, the existing of Cu NWs contributed to the enhanced light absorption of TiO_2 through the hydrogenating process.

In order to investigate the microstructure of black TiO_2, the samples were characterized by high resolution transmission electron microscopy (HRTEM), as shown in Fig. 2(a). Fringes of Cu NWs were clearly

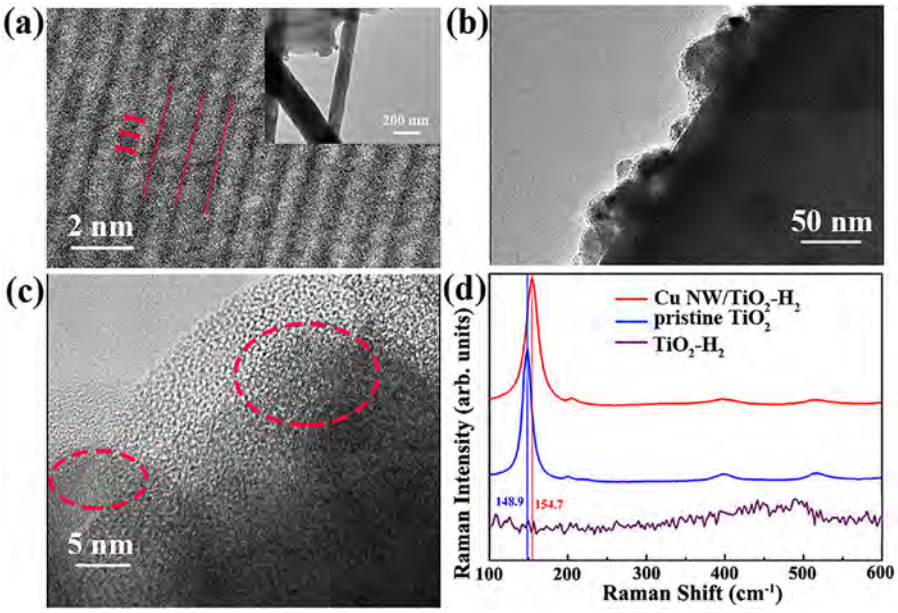

Fig. 2. (a) high-resolved TEM image of Cu NWs of selected region from inset image; (b) TEM image of TiO_2 nanoparticles along the Cu NWs; (c) TEM images of hydrogen treated TiO_2 nanoparticles; (d) Raman spectra of Cu NW/TiO_2—H_2, TiO_2—H_2 and pristine TiO_2.

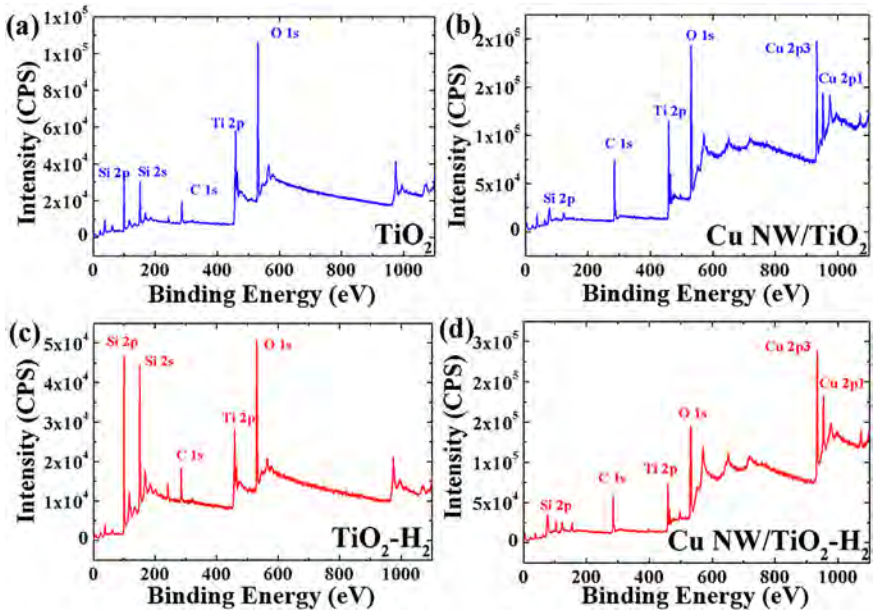

Fig. 3. XPS survey spectra of (a) TiO_2 film; (b) Cu NW/TiO_2 film; (c) TiO_2—H_2 film; (d) Cu NW/TiO_2—H_2 film.

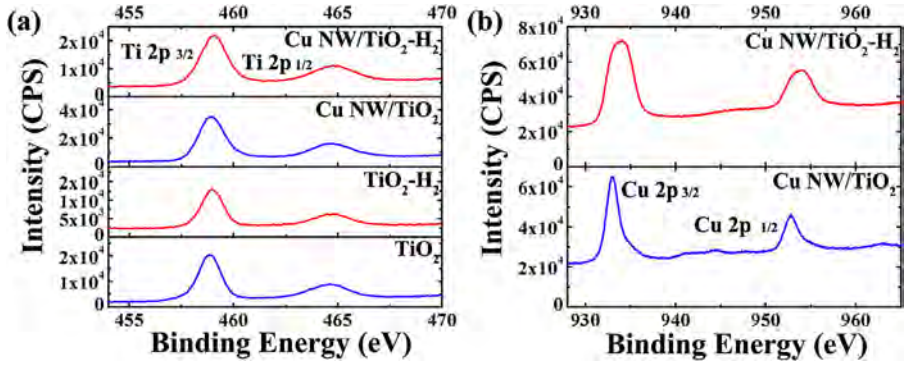

Fig. 4. (a) Ti 2p XPS spectra of the Cu NW/TiO_2—H_2 film, Cu NW/TiO_2 film, TiO_2—H_2 film and TiO_2 film. (b) Cu 2p XPS spectra of the Cu NW/TiO_2—H_2 film and Cu NW/TiO_2 film.

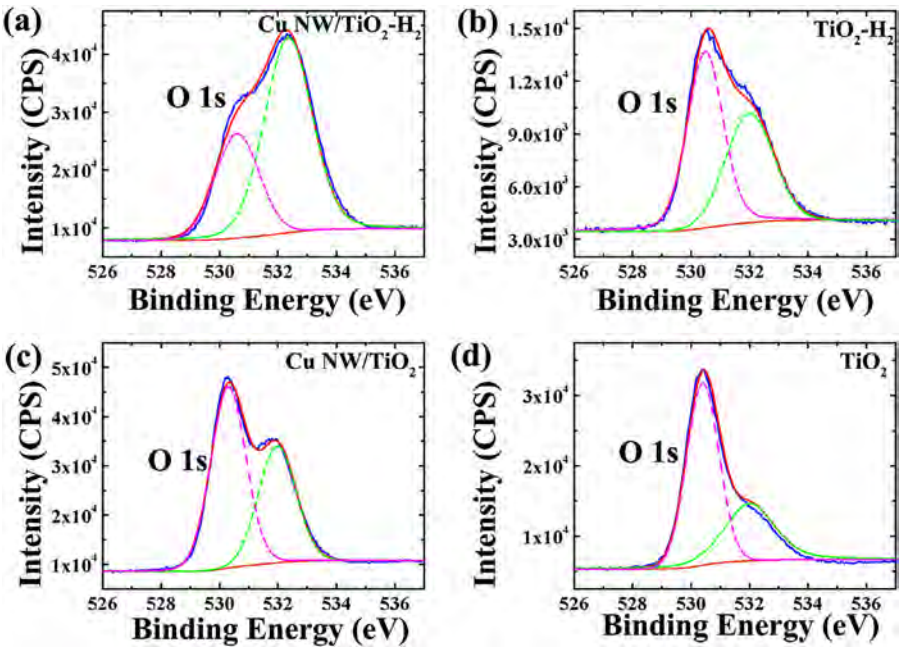

Fig. 5. Normalized O 1 s XPS spectra of (a) the Cu NW/TiO_2—H_2 film, (b) the TiO_2—H_2 film, (c) the Cu NW/TiO_2 film and (d) the TiO_2 film. The blue curve is the experimental result which deconvoluted into two peaks 530.4 eV (pink) and 532.0 eV (green). The red curve is the summation of the two deconvoluted peaks.

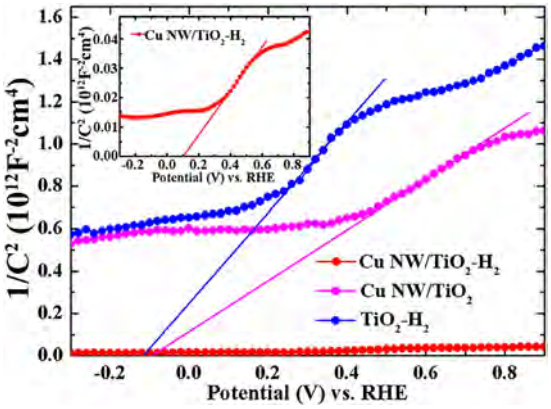

Fig. 6. Mott-Schottky plots collected at a frequency of 5 Hz in the dark for different samples.

observed in the selected regions, which was corresponding to the {111} planes along the axis of the nanowires [20]. Such observation indicated that the structure of Cu NWs networks was well maintained after the fabrication process. From Fig. 2(b) we can see that the TiO_2 nanoparticles gather along the Cu NWs, and the size is approximately 30–40 nm in diameter. After hydrogen treatment at 400 °C, TiO_2 becomes partially crystallized, as evidenced by the lattice fringes with different interplanar spaces appeared in Fig. 2(c) (circled out by red color), which are not consistent with the standard D-spacing of crystalline TiO_2. The TEM result showed that TiO_2 particles with crystalline/amorphous structure were generated in Cu NW/TiO_2—H_2 samples.

Raman spectroscopy was used to characterize the oxygen deficiency and amorphous surface of Cu NW/TiO_2–H_2 films. As shown in Fig. 2(d), the strongest Eg mode area of Cu NW/TiO_2—H_2 film at 144 cm^{-1} exhibited a blue shift (5.8 cm^{-1}) compared with pristine TiO_2, accompanying by a slight peak broadening (3 cm^{-1}). Bassi et al. reported that the existence of oxygen non-stoichiometry caused the blue shift of Eg mode [24]. Besides, TiO_2—H_2 films exhibited no obvious TiO_2 characteristic peak (Eg mode area), which indicated that without the assistance of Cu NWs, H_2 treatment could not lead to the structural transformation of TiO_2. The above results represent for the formation of oxygen deficiency and nonstoichiometric TiO_2 after hydrogen treatment on the surface of Cu NW/TiO_2—H_2 films, as reported in previous study [25].

In order to evaluate valence state change of elements in Cu NW/TiO_2 and TiO_2 film induced by hydrogen treatment, we further conducted X-ray photoelectron spectroscopy. From Fig. 3 we can reveal that XPS survey spectra of Cu NW/TiO_2 film has no significant change

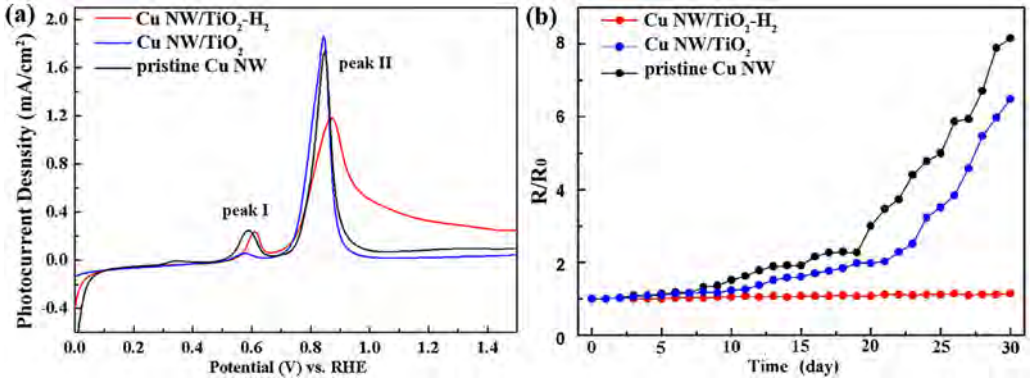

Fig. 7. Stability performance contrast of various samples, Cu NW/TiO_2–H_2 (red), Cu NW/TiO_2 (blue), pristine Cu NWs (black): (a) Linear sweeps voltammogram result; (b) Change of the resistance ratio (R/R0).

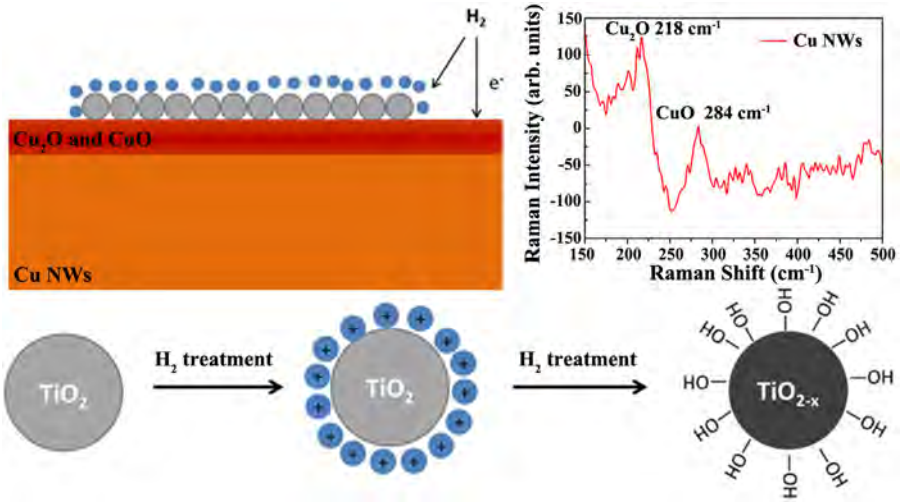

Scheme 1. Schematic diagram for the formation of defective nonstoichiometric TiO_2.

before and after hydrogen treatment, which is the same with that of TiO_2 film. Fig. 4(a) showed the Ti 2p spectra of Cu NW/TiO_2 films and TiO_2 films before and after hydrogen treatment. The treatment had no effect on the peak positions of Ti $2p_{1/2}$ and Ti $2p_{3/2}$ peak (centered at binding energies of 458.8 eV and 464.6 eV), and peak of Ti^{3+} were not found. The Ti 2p spectra characterization result is consistent with the typical Ti^{4+}-O bonds values for TiO_2 [22,23]. The O1s peak of the Cu NW/TiO_2–H_2 films exhibits great difference from that of the Cu NW/TiO_2 films, as shown in Fig. 5(a) and (c). The O1s peak can be deconvoluted into two peaks centered at 530.4 and 532.0 eV. The 532.0 eV peak is attributed to Ti-OH, which is ~1.5–2.0 eV higher than that of the O1s peak in TiO_2 (at ~530.4 eV). The stronger peak at 532.0 eV in Cu NW/TiO_2–H_2 films compared with that in Cu NW/TiO_2 films, confirmed the formation of hydroxyl groups on the surface of TiO_2 after hydrogen treatment [23]. As seen from Fig. 5(b) and (d), after the hydrogen treatment, the increase of peak at 532.0 eV in TiO_2 films is less than that in Cu NW/TiO_2 film, which again testified that Cu NW could assist the hydroxyl groups generation of TiO_2 during hydrogen treatment. The Cu 2p spectra of Cu NW/TiO_2 and Cu NW/TiO_2—H_2 films is shown in Fig. 4(b), which reveals that Cu NWs are not oxidized during the process of hydrogen treatment. Actually, a thin-layer of Cu_2O and CuO formed during the fabrication process of Cu NWs and Cu NW/TiO_2 film, as shown in Raman spectra of Scheme 1 [26,27]. When the films were treated in hydrogen environment, electron would transfer from H_2 to Cu(I), which resulted in hydrion and Cu(0). Subsequently, Ti-O-H was generated under the electrostatic attraction, and large numbers of hydroxyl groups formed on TiO_2 surface after the hydrogen treatment. Eventually, as shown in Scheme 1, nonstoichiometric TiO_2 with oxygen vacancies formed.

In order to calculate the carrier density and investigate the influence of hydrogen treatment on the TiO_2 electronic properties, the electrochemical impendence spectroscopy measurements were conducted on Cu NW/TiO_2–H_2, Cu NW/TiO_2 and TiO_2–H_2 films. All samples showed a positive slope in the Mott-Schottky plots, which is a typical characteristic of n-type semiconductor, as shown in Fig. 6. Importantly, the Cu NW/TiO_2–H_2 samples showed substantially smaller slopes of Mott-Schottky plot compared with the Cu NW/TiO_2 and TiO_2–H_2. The carrier densities of these samples were calculated from the slopes of Mott-Schottky plots using the equation:

$$N_d = (2/e_0\varepsilon_0\varepsilon)[d(1/C^2)/dV]^{-1} \quad (1)$$

Where e_0 is the electron charge($e_0 = 1.6 \times 10^{-19}$), ε is the dielectric constant of TiO_2 (ε = 170) [28], ε_0 is the permittivity of vacuum, N_d is the carrier density, and V is the applied bias at the electrode. The calculated carrier densitiy of the Cu NW/TiO_2–H_2 film is 1.126×10^{19} cm^{-3}, which is 25.3 times and 14.3 times larger than that of Cu NW/TiO_2 film (4.267×10^{17} cm^{-3}) and TiO_2–H_2 film (7.364×10^{17} cm^{-3}) respectively. It is revealed that hydrogen treatment with the assistance of Cu NWs led to a significant enhancement of carrier density in TiO_2. The enhanced carrier density is due to the increased oxygen vacancies, which are known to be an electron acceptor for TiO_{2-x}, and the increased carrier density improves the carrier transport in TiO_2.

The stability between three different films had been compared by analyzing electrochemical measurement results. There were two obvious peaks existing on the curve of hydrogen treated samples and other two reference samples. These two peaks represented for the electrochemical anodic process of copper element, oxidizing Cu to Cu_2O (peak I)and $Cu(OH)_2$ (peak II). The positions of Cu anodic peak in Cu NW/TiO_2 film almost kept the same with those in pristine Cu NWs film, which located at 0.58 V and 0.84 V vs RHE, as shown in Fig. 7(a). Differently, the Cu anodic peak positions of Cu NW/TiO_2–H_2 film upshifted to 0.61 V and 0.87 V vs RHE. According to the electrochemical principles, it can be derived that higher anodic peak position means the more stable species. Therefore, the 0.03 V upshift of Cu anodic peak position can reveal that Cu NWs in the Cu NW/TiO_2–H_2 films become more difficult to be oxidized during the linear voltage sweep process, and the generated TiO_2 films can play as a role of oxidation barrier to protect the under-lying Cu NWs. Stability test of the hybrid Cu NW/TiO_2 films with and without hydrogen treatment also has been done under the condition of 25 °C, 40% RH, as shown in Fig. 7(b). Resistances of Cu NW/TiO_2 and pristine Cu NW films increased rapidly, while the R/R0 of Cu NW/TiO_2–H_2 film was maintained below 1.2 for 30 days. The Cu NW/TiO_2–H_2 films showed excellent oxidation resistance, which was superior to the Cu NW/TiO_2 films and pristine Cu NW films. In our previous work, we had proved that oxidation firstly occurred at the Cu NW junction regions [29]. While during the hydrogen treatment process, The TiO_2 nanoparticles tended to aggregate around the nanowire and junction regions. When the Cu NW/TiO_2—H_2 film was exposed to atmosphere environment, O_2 and H_2O would react with TiO_{2-x} preferentially to generate TiO_2. So the black TiO_2-solderd junctions can help to improve the anti-oxidation stability of Cu NWs obviously.

4. Conclusion

In summary, hybrid copper nanowires-TiO_2 film with enhanced charge carrier properties has been fabricated by using atmospheric pressure hydrogen treatment method. Cu NWs with high electron transfer activity can promote the carrier transport in the hydrogenation process, which resulting in the generation of oxygen vacancies and

surface hydroxyl groups on TiO_2. The Cu NW/TiO_2–H_2 film exhibits a carrier density of 1.126×10^{19} cm^{-3}, which is about 25.3 times larger than that of the samples without hydrogen treatment

Declaration of Competing Interest

The authors declare no competing financial interest.

Acknowledgements

This work was supported by the National Key Research and Development Program of China (2016YFA0203000) and Instrument and equipment development program sponsored by Chinese Academy of Sciences (YJKYYQ20180065).

References

[1] X. Chen, S.S. Mao, Titanium Dioxide Nanomaterials, Synthesis, properties, modifications, and applications, Chem. Rev. 107 (2007) 2891–2959.
[2] A. Fujishima, K. Honda, Electrochemical photolysis of water at a semiconductor electrode, Nature 238 (1972) 37–38.
[3] M.R. Hoffmann, S.T. Martin, W. Choi, D.W. Bahnemann, Environmental applications of semiconductor photocatalysis, Chem. Rev. 95 (1995) 69–96.
[4] X. Lü, F. Huang, X. Mou, Y. Wang, F. Xu, A general preparation strategy for hybrid Tio_2 hierarchical spheres and their enhanced solar energy utilization efficiency, Advanced Materials 22 (2010) 3719–3722.
[5] X. Feng, K. Shankar, O.K. Varghese, M. Paulose, T.J. Latempa, C.A. Grimes, Vertically aligned single crystal Tio_2 nanowire arrays grown directly on transparent conducting oxide coated glass: Synthesis details and applications, Nano Lett. 8 (2008) 3781–3786.
[6] G.K. Mor, K. Shankar, M. Paulose, O.K. Varghese, C.A. Grimes, Enhanced photocleavage of water using titania nanotube arrays, Nano Lett. 5 (2004) 191–195.
[7] Y.J. Hwang, A. Boukai, P. Yang, High density n-Si/n-TiO_2 core/shell nanowire arrays with enhanced photoactivity, Nano Lett. 9 (2008) 410–415.
[8] Z.G. Zou, J.H. Ye, K. Sayama, H. Arakawa, Direct splitting of water under visible light irradiation with an oxide semiconductor photocatalyst, Nature 414 (2001) 625–627.
[9] A.L. Linsebigler, G. Lu, J.T. Yates, Photocatalysis on TiO_2 surfaces: Principles, mechanisms, and selected results, Chem. Rev. 95 (1995) 735–758.
[10] U. Diebold, The surface science of titanium dioxide, Surf. Sci. Rep. 48 (2003) 53–229.
[11] X.B. Chen, L. Liu, P.Y. Yu, S.S. Mao, Increasing solar absorption for photocatalysis with black hydrogenated titanium dioxide nanocrystals, Science 331 (2011) 746–750.
[12] G.M. Wang, H.Y. Wang, Y.C. Ling, Y.C. Tang, X.Y. Yang, R.C. Fitzmorris, C.C. Wang, J.Z. Zhang, Y. Li, Hydrogen-Treated TiO_2 nanowire arrays for photoelectrochemical water splitting, Nano Lett. 11 (2011) 3026–3033.
[13] A. Naldoni, M. Allieta, S. Santangelo, M. Marelli, F. Fabbri, S. Cappelli, C.L. Bianchi, R. Psaro, V. Dal Santo, Effect of nature and location of defects on bandgap narrowing in black TiO_2 nanoparticles, J. Am. Chem. Soc. 134 (2012) 7600–7603.
[14] X.H. Lu, G.M. Wang, T. Zhai, M.H. Yu, J.Y. Gan, Y.X. Tong, Y. Li, Hydrogenated TiO_2 nanotube arrays for supercapacitors, Nano Lett. 12 (2012) 1690–1696.
[15] Z. Wang, C. Yang, T. Lin, H. Yin, P. Chen, D. Wan, F. Xu, F. Huang, J. Lin, X. Xie, M. Jiang, Visible-light photocatalytic, solar thermal and photoelectrochemical properties of aluminium-reduced black titania, Energy Environ Sci 6 (2013) 3007.
[16] S. De, T.M. Higgins, P.E. Lyons, E.M. Doherty, P.N. Nirmalraj, W.J. Blau, J.J. Boland, J.N. Coleman, Silver nanowire networks as flexible, transparent, conducting films: Extremely high dc to optical conductivity ratios, ACS Nano 3 (2009) 1767–1774.
[17] H. Wu, L.B. Hu, M.W. Rowell, D.S. Kong, J.J. Cha, J.R. McDonough, J. Zhu, Y. Yang, M.D. McGehee, Y. Cui, Electrospun metal nanofiber webs as high-performance transparent electrode, Nano Lett. 10 (2010) 4242–4248.
[18] P.E. Lyons, S. De, J. Elias, M. Schamel, L. Philippe, A.T. Bellew, J.J. Boland, J.N. Coleman, High-Performance transparent conductors from networks of gold nanowires, Journal of Physical Chemistry Letters 2 (2011) 3058–3062.
[19] H. Zhang, K. Tan, H. Zheng, Y. Gu, W.F. Zhang, Preparation, characterization and photocatalytic activity of TiO_2 codoped with yttrium and nitrogen, Mater. Chem. Phys. 125 (2011) 156–160.
[20] D.Q. Zhang, R.R. Wang, M.C. Wen, D. Weng, X. Cui, J. Sun, H.X. Li, Y.F. Lu, Synthesis of ultralong copper nanowires for high-performance transparent electrodes, J. Am. Chem. Soc. 134 (2012) 14283–14286.
[21] X. Wang, L. j. Shi, R.R. Wang, J. Sun, Synthesis,Optimization of cu nanowires and application of its transparent electrodes, Journal of Inorganic Materials 34 (2019) 49–59.
[22] M.S. Lazarus, T.K. Sham, X-Ray photoelectron-spectroscopy (XPS) studies of hydrogen reduced rutile (TiO_{2-X}) surfaces, Chem. Phys. Lett. 92 (1982) 670–673.
[23] E. McCafferty, J.P. Wightman, Determination of the concentration of surface hydroxyl groups on metal oxide films by a quantitative xps method, Surface And Interface Analysis 26 (1998) 549–564.
[24] A. Li Bassi, D. Cattaneo, V. Russo, C.E. Bottani, E. Barborini, T. Mazza, P. Piseri, P. Milani, F.O. Ernst, K. Wegner, S.E. Pratsinis, Raman spectroscopy characterization of titania nanoparticles produced by flame pyrolysis: The influence of size and stoichiometry, J Appl Phys (2005) 98.
[25] J.C. Parker, R.W. Siegel, Raman microprobe study of nanophase TiO_2 and oxidation-induced spectral changes, J Mater Res 5 (1990) 1246–1252.
[26] S.L. Shinde, K.K. Nanda, Facile synthesis of large area porous Cu2O as super hydrophobic yellow-red phosphors, RSC Adv 2 (2012) 3647–3650.
[27] B.L. Hurley, R.L. McCreery, Raman spectroscopy of monolayers formed from chromate corrosion inhibitor on copper surfaces, J. Electrochem. Soc. 150 (2003) B367–B373.
[28] R.A. Parker, Static dielectric constant of rutile (TIO_2), 1.6-1060 degrees k, Physical Review 124 (1961) 1719–1722.
[29] L.J. Shi, R.R. Wang, H.T. Zhai, Y.Q. Liu, L. Gao, J. Sun, A long-term oxidation barrier for copper nanowires: graphene says yes, Physical Chemistry Chemical Physics 17 (2015) 4231–4236.